DOI: 10.1002/chem.200801578

Total Syntheses of Casuarine and Its 6-*O*-α-Glucoside: Complementary Inhibition towards Glycoside Hydrolases of the GH31 and GH37 Families

Francesca Cardona,[a] Camilla Parmeggiani,[a] Enrico Faggi,[a] Claudia Bonaccini,[b] Paola Gratteri,[b] Lyann Sim,[c] Tracey M. Gloster,[d] Shirley Roberts,[d] Gideon J. Davies,[d] David R. Rose,[c] and Andrea Goti*[a]

Abstract: Total synthesis of naturally occurring casuarine (**1**) and the first total synthesis of casuarine 6-*O*-α-glucoside (**2**) were achieved through complete stereoselective nitrone cycloaddition, Tamao–Fleming oxidation and selective α-glucosylation as key steps. Biological assays of the two compounds proved their strong and selective inhibitory properties towards glucoamylase NtMGAM and trehalase Tre37A, respectively, which place them among the most powerful inhibitors of these enzymes. The structural determination of the complexes of NtMGAM with **1** and of Tre37A with **2** revealed interesting similarities in the catalytic sites of these two enzymes which belong to different families and clans.

Keywords: enzyme structures · maltase glucoamylase · natural products · total synthesis · trehalase

Introduction

Casuarine, (1*R*,2*R*,3*R*,6*S*,7*S*,7a*R*)-3-(hydroxymethyl)-1,2,6,7-tetrahydroxypyrrolizidine (**1**), and its 6-*O*-α-glucoside, casuarine 6-*O*-α-glucopyranoside (**2**) (see below), have been isolated from the bark of *Casuarina equisetifolia* L. (Casuarinaceae) and from the leaves of *Eugenia jambolana* Lam. (Myrtaceae),[1] two plants well known for their therapeutic action against diarrhoea, dysentery and colic,[2] breast cancer,[1] diabetes and bacterial infections.[2,3] Compounds **1** and **2** are strong inhibitors of the fungal glucoamylase from

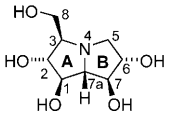

1

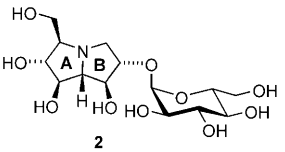

2

Aspergillus niger, with very similar IC_{50} values ($IC_{50}=0.7$ μM for **1**, $IC_{50}=1.1$ μM for **2**).[4] No inhibition data against human α-glucosidases or glucoamylases are available to date.

Human maltase-glucoamylase (MGAM, EC 3.2.1.20) falls into family GH31 of the Carbohydrate Active enZyme (CAZy) classification.[5] It is one of the two enzymes (together with sucrase-isomaltase SI, EC 3.2.1.48 and 3.2.1.10) responsible for catalyzing the last step in starch digestion by hydrolyzing mixtures of dextrins at the non-reducing end into glucose with net retention of anomeric configuration.[6] Inhibitors of enzymes involved in the starch-digestion pathway are used to delay glucose production and thus aid in the treatment of Type II diabetes.[7] This therapeutic poten-

[a] Dr. F. Cardona, C. Parmeggiani, Dr. E. Faggi, Prof. A. Goti
Department of Organic Chemistry "U. Schiff"
Laboratory of Design, Synthesis
and Study of Biologically Active Heterocycles (HeteroBioLab)
University of Florence, Via della Lastruccia, 13
50019 Sesto Fiorentino (FI) (Italy)
Fax: (+39) 055-457-3531
E-mail: andrea.goti@unifi.it

[b] Dr. C. Bonaccini, Prof. P. Gratteri
Laboratory of Molecular Modeling
Cheminformatics & QSAR, Department of Pharmaceutical Sciences
Laboratory of Design, Synthesis
and Study of Biologically Active Heterocycles (HeteroBioLab)
University of Florence, Via U. Schiff 6
50019 Sesto Fiorentino (FI) (Italy)

[c] L. Sim, Prof. D. R. Rose
Ontario Cancer Institute and Department of Medical Biophysics
University of Toronto, 101 College St., Toronto M5G 1L7 (Canada)

[d] Dr. T. M. Gloster, S. Roberts, Prof. G. J. Davies
York Structural Biology Laboratory, Department of Chemistry
University of York, Heslington, York, YO10 5YW (UK)

Supporting information for this article is available on the WWW under http://dx.doi.org/10.1002/chem.200801578: Experimental procedures and characterization for compounds **7**, **12**, **13**, and **14**, the acetate derivative of **9** and the diacetate derivative of **10**, and ^1H and ^{13}C NMR spectra of all compounds.

 © 2009 Wiley-VCH Verlag GmbH & Co. KGaA, Weinheim

tial would be encouraged by an in-depth study of their mode of action.[8] Some of us recently reported[9] the first crystal structure of the human *N*-terminal subunit of MGAM (NtMGAM) in its apo form and in complex with acarbose (**3**) (see below), a tetrasaccharide analogue currently on the market as an antidiabetic drug (Glucobay, Precose).

Trehalases, another class of glycoside hydrolase of current interest, hydrolyze one of the two glycosidic bonds in trehalose (α-D-glucopyranosyl-α-D-glucopyranoside) with inversion at the anomeric center.[10] Trehalases are vital for insect flight by providing glucose from trehalose hydrolysis, and thus their inhibition is an interesting target for novel insecticides.[7] Casuarine (**1**) and its glucoside **2** are known to inhibit porcine kidney trehalase ($IC_{50}=12$ and 0.34 μM, respectively).[4] Some of us recently presented the first three-dimensional structure of a periplasmic trehalase from *Escherichia coli* (Tre37A), which belongs to family GH37 of the CAZy classification, in complex with some potent inhibitors, 1-thiatrehazolin (**4**) and validoxylamine A (**5**).[11] In order to evaluate and compare the inhibitory activity of **1** and **2** towards the human NtMGAM and *E. coli* Tre37A we undertook the total syntheses of both compounds.

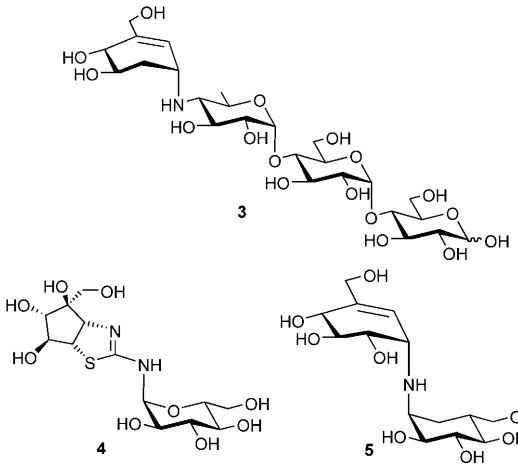

Isolation and purification of **1** and **2** from natural sources are very difficult and expensive, and afford only minor amounts (indeed, **2** has never been obtained in a chemically pure form). Furthermore, very few total syntheses of casuarine (**1**) have been reported to date,[12,13] and no total synthesis of **2** has been previously described. The highly complex and challenging structure of casuarine, as it is the most highly hydroxylated pyrrolizidine alkaloid and possesses six contiguous carbon stereocenters, is presumably responsible for the limited number of synthetic approaches described. An additional problematic issue in the synthesis of casuarine 6-*O*-α-glucoside lies in the selectivity of glucosylation of the hydroxy group at C6. Carefully planned extraction procedures have recently uncovered more examples of glycosyl iminosugars isolated from natural sources, thus indicating that their occurrence in Nature is not uncommon.[14] In contrast, few syntheses of glycosyl iminosugars are reported in the literature,[15,16] and they all reflect some difficulties in targeting the final compounds with good yields and selectivities, particularly in the glucosylation step. Interestingly, their inhibitory properties differ substantially from those of the parent iminosugar, with the linked carbohydrate moiety usually generating higher selectivity. This can be due, in principle, to a different arrangement within the catalytic site or, most likely, to additional stabilizing (or destabilizing) interactions with other subsites.

In this paper we report a straightforward and highly selective approach to the synthesis of casuarine (**1**) and the first total synthesis of casuarine-6-*O*-α-glucoside (**2**), their inhibitory activity towards NtMGAM and Tre37A, and the three-dimensional structure of NtMGAM in complex with **1** and Tre37A in complex with **2**, supported by a molecular modeling study. These data provide a rationale for understanding the complementary inhibitory properties of **1** and **2** against human NtMGAM and *E. coli* Tre37A. These studies also show that although MGAM and Tre37A belong to different families and clans,[5] have different sizes, and operate by different mechanisms (MGAM proceeds with retention, and Tre37A with inversion of configuration at the anomeric center), many similarities are found within their active sites. Importantly, we found that casuarine (**1**) is able to inhibit NtMGAM more strongly than the pseudo tetrasaccharide acarbose (**3**), holding promise for the development of novel antidiabetic drugs, and that its 6-*O*-α-glucoside **2** inhibits Tre37A at levels comparable with its most powerful known inhibitors.

Results and Discussion

Our approach to the synthesis of casuarine (**1**) started with nitrone **6**, available in multigram scale from 2,3,5-tri-*O*-benzylarabinofuranose.[17] Nitrone **6** has the correct relative and absolute stereochemistry at C1, C2 and C3 of the target molecule. The first key step for the synthesis of the casuarine skeleton was the 1,3-dipolar cycloaddition of nitrone **6** with (*Z*)-alkene **7**. Although no close example was reported, we were confident that (*Z*)-disubstituted alkene **7** could provide the correct regioselectivity in the cycloaddition step on the basis of related nitrone cycloadditions with vinyl silanes.[18] Indeed, the desired adduct **8** was obtained with high regio- and stereoselectivity in 79% yield (Scheme 1). The regiochemistry and relative stereochemistry of **8** were firmly established on the basis of COSY and NOESY experiments. The complete stereoselectivity of the 1,3-dipolar cycloaddition, which allowed the selective installation of the three new stereocenters (corresponding to C6, C7 and C7a in the target molecule) in one step with the required configuration, may be ascribed to the peculiar all-*trans* disposition of the benzyloxy groups in nitrone **6**, which hampered any *endo* or *syn* approaches.[17,19]

 © 2009 Wiley-VCH Verlag GmbH & Co. KGaA, Weinheim

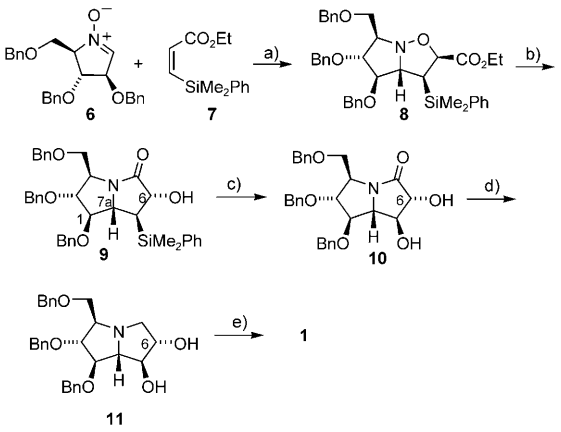

Scheme 1. Synthesis of casuarine (**1**). a) CH_2Cl_2, RT, 36 h, 79%; b) Zn, AcOH/H_2O, 60–65°C, 5 h, 93%; c) $Hg(CF_3CO_2)_2$, TFA, AcOH, AcOOH, $CHCl_3$, 76%; d) $LiAlH_4$, THF, reflux, 78%; e) H_2, Pd/C, MeOH, HCl, 100%.

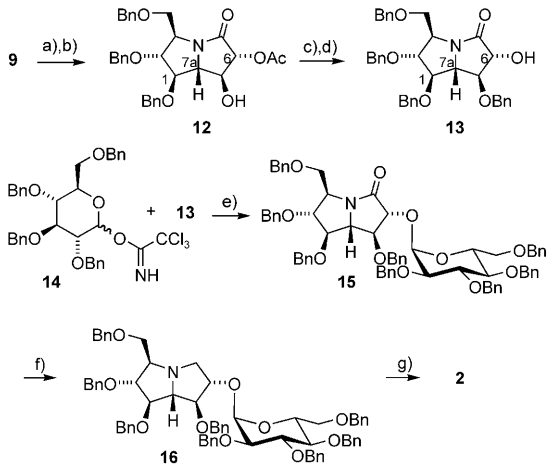

Scheme 2. Synthesis of casuarine 6-*O*-α-glucoside (**2**). a) Ac_2O, Py, RT, 15 h, 100%; b) $Hg(CF_3CO_2)_2$, TFA, AcOH, AcOOH, $CHCl_3$, 82%; c) $BnOC(=NH)CCl_3$, CF_3SO_3H, Et_2O, RT, 3 h; d) Ambersep 900 OH, MeOH, RT, 15 h, 75% (2 steps); e) TMSOTf, Et_2O, −20°C, 40 min, 72%; f) $LiBH_4$, BH_3·THF, THF, 23°C, 3 d, 68%; g) H_2, Pd/C, MeOH, HCl, 77%.

Reductive cleavage of the N−O bond[17,20,21] with Zn in acetic acid followed by spontaneous *N*-cyclization afforded lactam **9** in 93% yield. Then, the Tamao–Fleming reaction[22] allowed oxidation of the C−Si bond with retention of configuration and 76% yield of diol **10**. Oxidation of the C-Si bond to C-OH with retention of configuration was confirmed by NOESY experiments performed on the diacetyl derivative of **10**. Finally, reduction of **10** with $LiAlH_4$ in refluxing THF (78% yield), followed by catalytic hydrogenation of pyrrolizidine **11**, provided quantitatively casuarine (**1**) as a white solid (m.p. 180–182°C). The spectroscopic data and physicochemical properties of the synthesized compound were identical to those of natural casuarine.[1a] Synthetic **1** showed a specific optical rotation ($[\alpha]_D^{20} = +14.4$ ($c = 0.52$, H_2O)) in good agreement with those reported for the natural and for the previously synthesized compound ($[\alpha]_D^{24} = +16.9$ ($c = 0.80$, H_2O);[1a] $[\alpha]_D^{27} = +10.8$ ($c = 1.02$, H_2O)[12a]). In conclusion, our total synthesis furnished casuarine in five steps and 44% overall yield from nitrone **6**, which compares well with the previously reported syntheses.

For the synthesis of casuarine 6-*O*-α-glucoside (**2**), we needed to carry out the Tamao–Fleming oxidation prior to glycosylation as the glycosidic bond did not tolerate the harsh reaction conditions of Tamao–Fleming oxidation. Acetylation of lactam **9** and subsequent Tamao–Fleming oxidation afforded **12** with 82% yield (Scheme 2). Then, a protection–deprotection sequence (75% yield over 2 steps) was required to give the intermediate **13**, which bears the free hydroxy group at C6 suitable to be linked to the glucose moiety. The glucosylation reaction of **13** was carried out with the trichloroacetimidate **14** and catalytic TMSOTf in diethyl ether and afforded selectively the α-anomer **15** in 72% yield. Only traces of the β-anomer, which could not be isolated, were detected in the crude reaction mixture. Reduction of C=O double bond of **15** was not a trivial task. $LiAlH_4$, Red-Al, $BH_3{\cdot}SMe_2$ or $LiBH_4$ in refluxing THF afforded complex mixtures of products, while at room temperature the starting material was converted only marginally. Eventually, treatment of **15** with a high excess of $LiBH_4$ in combination with BH_3·THF at room temperature for three days[23] afforded glucoside **16** in 68% yield. Catalytic hydrogenation finally provided casuarine 6-*O*-α-glucoside (**2**) in 77% yield as a white foam.

The synthesis of casuarine 6-*O*-α-glucoside (**2**) renders it available in a chemically pure form. Indeed, the sample isolated from a natural source was evaluated to be only around 60% pure.[1b] Only ^1H NMR and ^{13}C NMR data have been reported for the isolated natural compound and they are in good agreement with those of the compound synthesized by us, thus confirming the assignment proposed by the authors.[1b]

Inhibition studies of **1** and **2** towards NtMGAM and Tre37A show complementary behaviour with the two enzymes (Table 1).

Table 1. Inhibition of NtMGAM and Tre37A by **1** and **2**.

	NtMGAM K_i	Tre37A K_i
casuarine (**1**)	0.45 μM	17 μM
casuarine 6-*O*-α-glucopyranoside (**2**)	280 μM	12 nM

NtMGAM inhibition studies revealed that **1**, with a K_i of 0.45 μM, displayed over 600-fold greater inhibition against NtMGAM compared to **2**, which inhibited with a K_i of 280 μM. These results are similar to the inhibition profile of rat intestinal maltase where **1** and **2** inhibit with IC_{50} values of 0.7 and 260 μM, respectively, but are in contrast to the inhibition profile of fungal glucoamylases where **1** and **2** display similar and potent inhibitory activities.[4]

The similarity in inhibition profiles between NtMGAM and the rat intestinal maltase agrees with previous kinetic

 © 2009 Wiley-VCH Verlag GmbH & Co. KGaA, Weinheim

studies,[9,24] which propose that the *N*-terminal MGAM domain of human maltase-glucoamylase displays maltase activity whereas its *C*-terminal catalytic domain displays glucoamylase activity.

The crystal structure of NtMGAM in complex with **1** was solved to 2.1 Å (see Experimental Section for details and data processing and refinement statistics). The electron density clearly revealed one molecule of **1**, Figure 1a, bound in

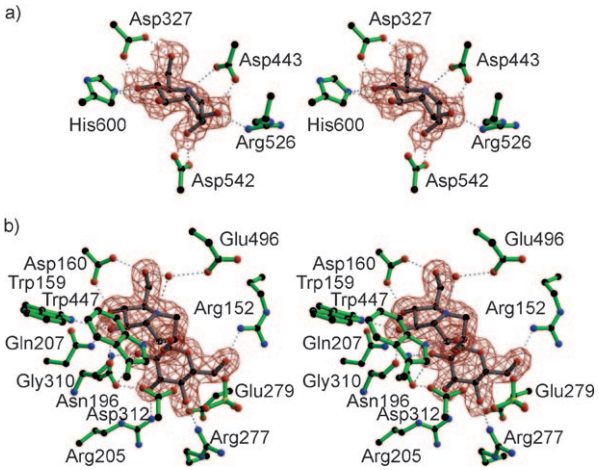

Figure 1. Stereo (divergent) ball-and-stick representation of a) casuarine (**1**) in complex with NtMGAM and b) casuarine 6-*O*-α-glucoside (**2**) in complex with Tre37A. Observed electron density for the maximum likelihood weighted $2F_{obs}-F_{calcd}$ map is contoured at 1σ; drawn by using BOBSCRIPT.[25]

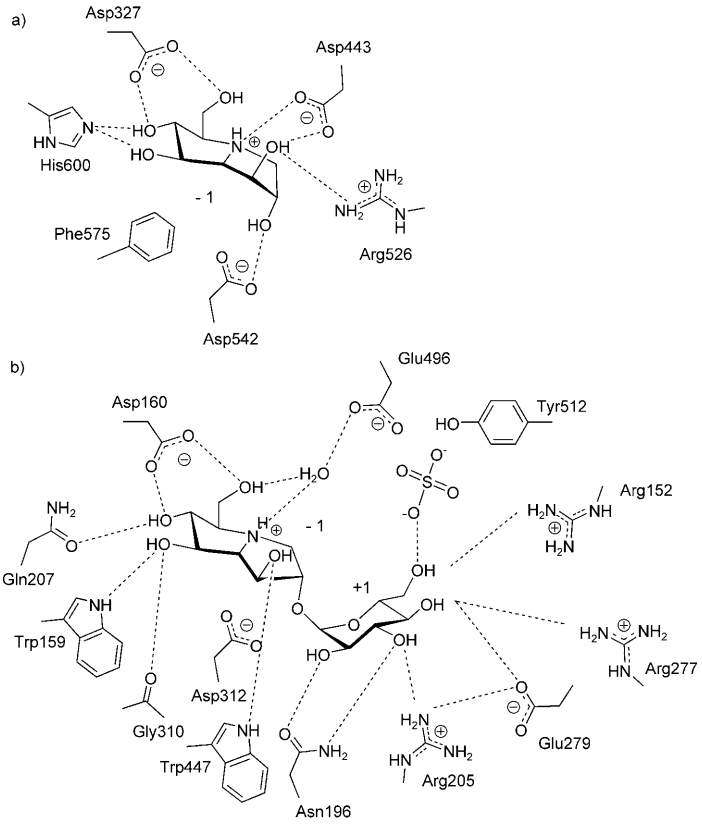

Figure 2. Interactions between a) **1** and NtMGAM (D443 is the catalytic nucleophile, D542 the catalytic acid/base) and b) **2** and Tre37A (E496 is the catalytic base, D312 the catalytic acid). Hydrogen bonds are shown by dashed lines.

the −1 subsite and one glycerol molecule (originating from the cryoprotection solution) bound in the +1 subsite. The two pyrrolidine rings, named "A" and "B" (shown above), both adopt an envelope configuration; ring A is in a ^2E conformation, and ring B in an E_6 conformation. With its heavily hydroxylated rings, **1** binds tightly to the NtMGAM active site primarily through hydrogen-bonding interactions with the side chains lining the −1 subsite (Figure 2a). These include hydrogen bonds between D327 and the hydroxyl groups at C8 and C2, H600 with the C1-OH and C2-OH, D443 with the C7-OH and the pyrrolidine nitrogen, R526 with the C7-OH and D542 with the C6-OH. The weaker inhibition of **2** compared with **1** leads us to believe that the addition of glucoside group of **2** makes unfavourable interactions with the +1 subsite, or weakly competes with the casuarine group to occupy the −1 subsite, both of which may decrease the inhibition properties of the casuarine group.

Kinetic data were measured on Tre37A using an assay where glucose was detected by glucose oxidase/peroxidase linking enzymes following trehalose hydrolysis (see Experimental Section for details). K_i values for **1** and **2** were determined at 37 °C and pH 5.5, and included a 20-minute pre-incubation of the inhibitor with the enzyme to prevent any complications in the data analysis from slow onset inhibition. Compound **2** was shown to be around a thousand fold more potent than **1** (Table 1), indicating that the glucose moiety in the +1 subsite (see below) contributes considerably to binding. This fits with the fact that Tre37A hydrolyses disaccharide substrates and therefore presumably has evolved to optimise interactions in both the −1 and +1 subsites.[11]

X-ray data for Tre37A in complex with **2** were collected to 1.9 Å (see Experimental Section for details and data processing and refinement statistics). There was clear electron density in each of the four molecules of the asymmetric unit corresponding to a molecule of **2**, Figure 1b. The casuarine moiety of **2** is bound in the −1 subsite of Tre37A (Figure 2b). The two pyrrolidine rings are both found in an envelope conformation; ring A is in a ^2E conformation, and ring B in a ^5E conformation. The glucose moiety of **2**, in the +1 subsite, is bound in a relaxed $^4C_1$ conformation. The majority of the interactions between the glucose and the active site residues of Tre37A are as described previously;[11] the exception to this is the hydroxyl group at the C6 position, which hydrogen bonds with a sulfate group from the crystallization conditions, and appears to cause a large movement of E511 away from the active site. The hydroxyl group at C8 of the casuarine moiety hydrogen bonds with D160 and a water molecule, the C2-OH interacts with D160 and the oxygen of Q207 and the C1-OH with W159 and the back-

 © 2009 Wiley-VCH Verlag GmbH & Co. KGaA, Weinheim

bone carbonyl of G310. The nitrogen atom in the pyrrolizidine ring interacts with the same water molecule as the C8-OH. In ring B, the hydroxyl group at C7 interacts with W447 and a different water molecule (not shown).

Despite having different protein sequences and architectural folds, structural comparison of the two enzymes reveals an intriguing similarity of their binding sites, as shown in Figure 3, which was obtained by overlapping the pyrrolizidine nuclei in the two enzyme–inhibitor complexes. Although not perfectly superimposable, almost every residue lining the −1 subsite of NtMGAM corresponds to a similar and analogously oriented residue in the Tre37A active site. The most conserved residues are those directly involved in ligand hydrogen bonding (D327, H600 and D542 in NtMGAM, which corresponds to D160, W159 and D312 in Tre37A, respectively). An exception to this is the backbone carbonyl of G310 in Tre37A, which corresponds to a water molecule in NtMGAM. Most of the hydrophobic residues lining the −1 subsite are also conserved and occupy approximately the same positions (Y299, W406, W441, W539 and H600 in NtMGAM which correspond to Y157, F153, W520, W447 and W159 in Tre37A, respectively). The two binding sites differ in the position of the catalytic side chains (D443, the nucleophile in the retaining NtMGAM and E496, the base in the inverting Tre37A), by more than 3 Å, reflecting the different mechanisms utilised by the enzymes. Strikingly, as mentioned above, the respective catalytic acids, D542 in MGAM and D312 in Tre37A, superimpose closely. An important difference between the two binding sites is the presence of a phenylalanine (F575) in NtMGAM in close proximity to the catalytic acid/base D542, while the corresponding amino acid in Tre37A is an alanine (A307). In accordance with their varying functions, the +1 binding sites of NtMGAM and Tre37A have major differences, reflecting the specificity for α-1,4 and α,α-1,1 linkages, respectively. In addition, this site in NtMGAM is exposed to the solvent, while in Tre37A it is a buried cavity.

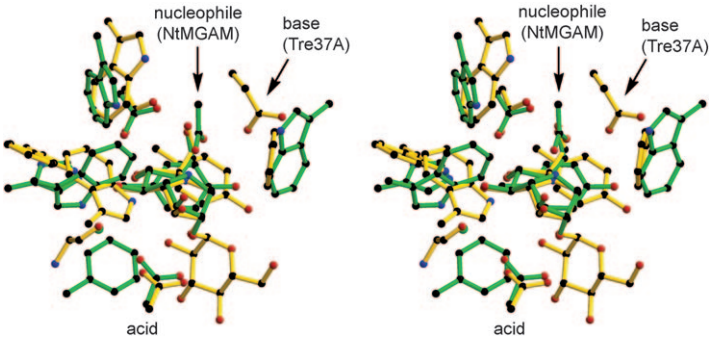

Figure 3. Stereo (divergent) ball-and-stick representation of active site overlap between NtMGAM in complex with **1** (green) and Tre37A in complex with **2** (yellow); drawn by using BOBSCRIPT.[25]

With the aim of rationalizing the binding data, we modeled the structure of NtMGAM in complex with casuarine 6-*O*-α-glucoside (**2**) and Tre37A in complex with casuarine (**1**) using Glide[26] docking simulations.

Docking of **2** in NtMGAM places the casuarine moiety in the −1 subsite, and consequently the glucose moiety in the +1 subsite (Figure 4c). With respect to the crystallographic structure (Figure 4a), the casuarine (aglyconic) portion of **2** is not perfectly overlapped with **1**, probably due to the presence of the 1,1-linkage instead of 1,4 present in physiological substrates. Nevertheless, all of the hydrogen bonds we found in the casuarine complex are formed by the casuarine portion of **2** in the modelling, with the exception of the hydrogen bond between C6-OH of casuarine and D542, because of the presence of the glucosidic bond in that position. The glucose moiety which lies in the +1 subsite is able to form a few hydrogen bonds with solvent exposed residues but is also in close contact to bulky residues that surround the −1 subsite entrance and which may form a sort of "linkage selector" in order to assure 1,4-linkage selectivity for the enzyme. All together, these observations give a rationale to the observed difference in inhibitory activity between **1** and **2**; the weaker inhibition of NtMGAM by **2** most likely reflects the specificity of the enzyme which has evolved to hydrolyse the α-1,4 linkages in starch-derived dextrins whereas **2** is a trehalose (α,α-1,1) mimic. Interestingly, a comparison with the crystal structure of NtMGAM in complex with acarbose previously reported,[9] shows that the acarbose (**3**) is stabilized by an electrostatic interaction between its positively charged nitrogen and D542, but lacks the two hydrogen bonds with D443 (Figure 4b). Therefore, casuarine (**1**) is the only one of the three inhibitors to interact with both of the key residues D443 and D542, which may be partly responsible for the two orders of magnitude increase in inhibition with respect to acarbose (**3**) or **2**.

Tre37A has a buried cavity, specific both for the α,α-1,1 substrate and for a glucoside in the +1 leaving group subsite. The shape and dimension of **2** are thus optimal for maximizing transition state mimicking interactions in the −1 subsite and leaving group glycoside interactions in +1. These are achieved through hydrogen bonds involving all of its acceptor and donor groups (Figure 5a). A similar network of interactions were observed for previously solved complexes with 1-thiatrehazolin (**4**) and validoxylamine A (**5**),[11] which have a similar enzyme affinity (Figure 5b and c, respectively). As the binding of **1** leaves one of the two subsites of Tre37A empty (Figure 5d and e), fewer hydrogen bonds can be formed with the protein. The formation of fewer interactions gives a rationalization for the lower affinity of the "monosaccharide-like" inhibitor compound as opposed to the "disaccharide-like" equivalent.

Conclusion

In summary, a straightforward total synthesis of casuarine (**1**) from nitrone **6** in five steps and 44% overall yield has been achieved, which featured complete stereoselective cycloaddition and Tamao–Fleming oxidation. This strategy al-

 © 2009 Wiley-VCH Verlag GmbH & Co. KGaA, Weinheim

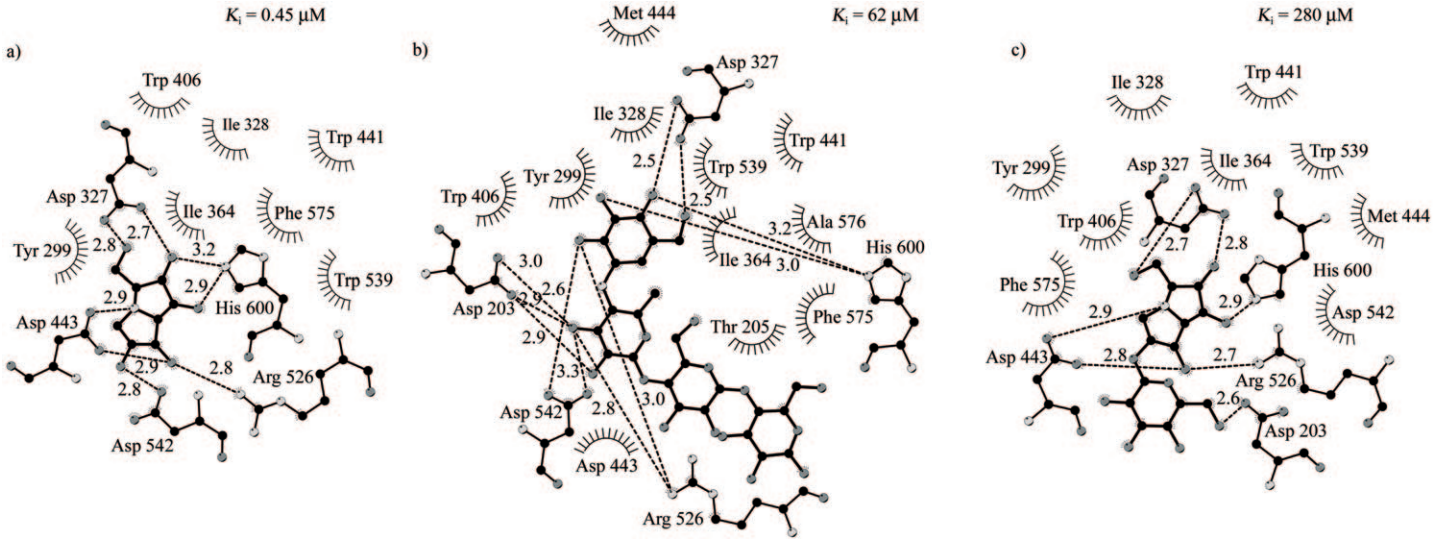

Figure 4. Schematic views of interactions between NtMGAM and a) casuarine (**1**) and b) acarbose (**3**) in the solved structures, and c) casuarine 6-*O*-α-glucoside (**2**) after docking. Plots were prepared with Ligplot.[27]

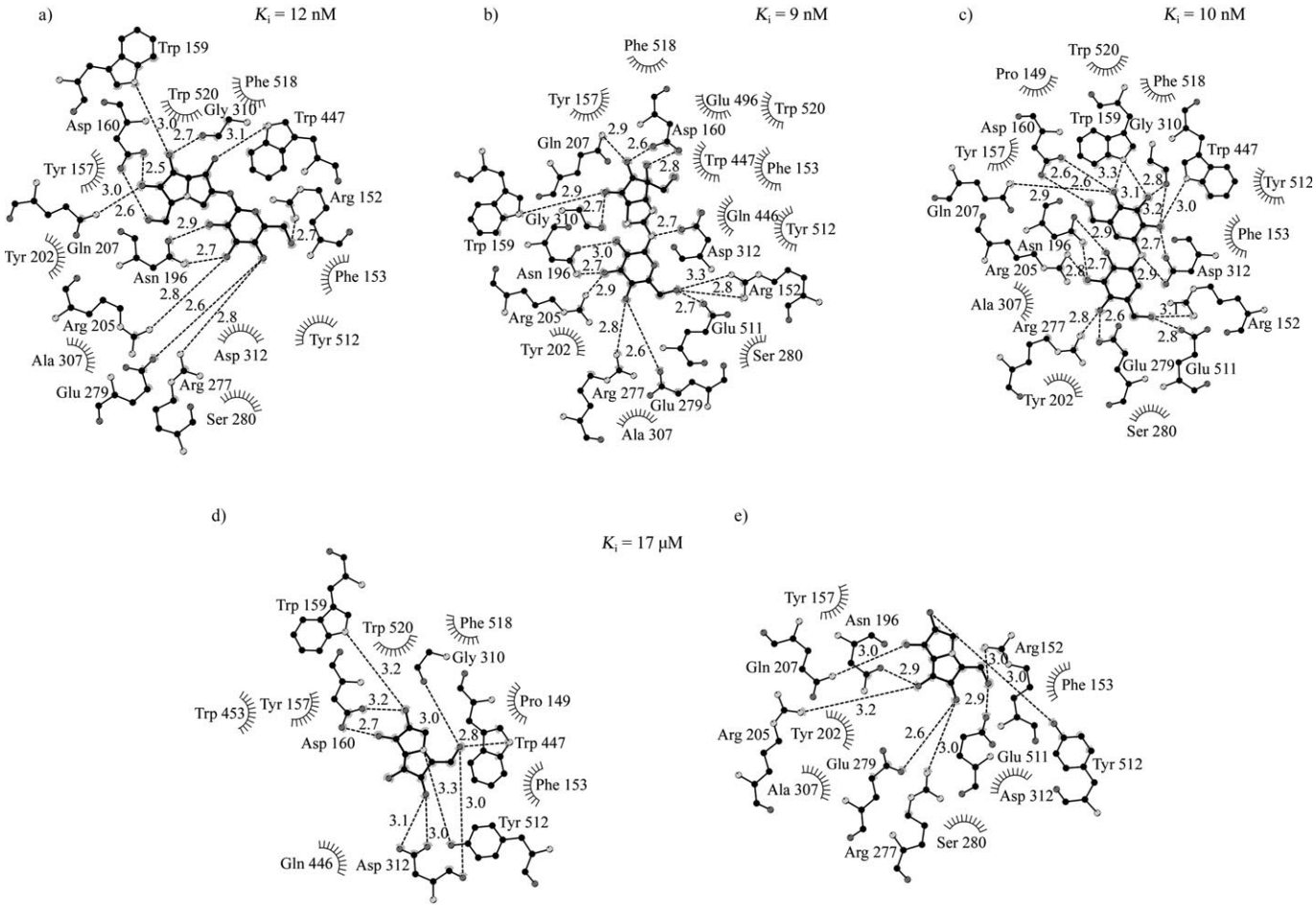

Figure 5. Schematic views of interactions between Tre37A and a) casuarine 6-*O*-α-glucoside (**2**), b) 1-thiatrehazolin (**4**) and c) validoxylamine A (**5**) in the solved structures and the two possible orientations of casuarine (**1**) after docking (d and e in −1 and +1 subsite, respectively). Plots were prepared with Ligplot.[27]

 © 2009 Wiley-VCH Verlag GmbH & Co. KGaA, Weinheim

lowed the total synthesis of casuarine 6-*O*-α-glucoside (**2**) to be accomplished from nitrone **6** in nine steps and 17% overall yield, thus opening the way for the generation of a number of differently glycosylated pyrrolizidine iminodisaccharides.

This study demonstrates that among glycoside hydrolase enzymes that belong to different families and clans, and which differ in mechanism of action, there is a degree of conservation of the analogous active site residues reflecting the convergent evolution of optimised non-covalent interactions. The binding of inhibitors **1** and **2** were investigated with NtMGAM and Tre37A by kinetic and structural methods, which provide information on the relevant interactions in the active site and could form the basis for the synthesis of analogues. This study shows that casuarine can be envisaged as a lead compound for the construction of novel disaccharide and polysaccharide type glycoside hydrolase inhibitors, the syntheses of which are currently ongoing in our laboratories.

Experimental Section

General methods: Commercial reagents were used as received. All reactions were magnetically stirred and monitored by TLC on 0.25 mm silica gel plates (Merck F_{254}) and column chromatography was carried out on Silica Gel 60 (32–63 μm). Yields refer to spectroscopically and analytically pure compounds unless otherwise stated. ^{1}H NMR spectra were recorded on a Varian Mercury-400. ^{13}C NMR spectra were recorded on a Varian Gemini-200. Infrared spectra were recorded with a Perkin-Elmer Spectrum BX FT-IR System spectrophotometer. Mass spectra were recorded on a QMD 1000 Carlo Erba instrument by direct inlet; relative percentages are shown in brackets. ESI full MS were recorded on a Thermo LTQ instrument by direct inlet; relative percentages are shown in brackets. Elemental analyses were performed with a Perkin-Elmer 2400 analyzer. Optical rotation measurements were performed on a JASCO DIP-370 polarimeter.

Ethyl (2*S*,3*S*,3a*S*,4*R*,5*R*,6*R*)-4,5-bis(benzyloxy)-6-(benzyloxy)methyl-3-[dimethyl(phenyl)silyl]-hexahydropyrrolo[1,2-*b*]isoxazole-2-carboxylate (8): A solution of nitrone **6**[17] (1.23 g, 2.95 mmol) and **7** (1.17 g, 6.16 mmol) in CH_2Cl_2 (3 mL) was stirred at RT for 36 h, then the solvent was removed under reduced pressure. Purification of the residue by chromatography on silica gel (petroleum ether/ethyl acetate 7:1) afforded pure **8** (1.52 g, 2.33 mmol, 79%) as a colorless oil. R_f=0.22 (petroleum ether/ethyl acetate 7:1). $[\alpha]_D^{22}=-76.6$ (c=0.56 in $CHCl_3$); ^{1}H NMR (400 MHz, $CDCl_3$, 25°C): δ=7.47–7.44 (m, 2H; H-Ar), 7.38–7.24 (m, 15H; H-Ar), 7.21–7.17 (m, 3H; H-Ar), 4.85 (d, ^3J=8.8 Hz, 1H; H2), 4.58 (A part of an AB system, ^2J=12.2 Hz, 1H; Bn), 4.55 (B part of an AB system, ^2J=12.2 Hz, 1H; Bn), 4.39 (A part of an AB system, ^2J=11.9 Hz, 1H; Bn), 4.33 (B part of an AB system, ^2J=11.9 Hz, 1H; Bn), 4.24 (A part of an AB system, ^2J=12.0 Hz, 1H; Bn), 4.16 (B part of an AB system, ^2J=12.0 Hz, 1H; Bn), 4.05–3.90 (m, 4H; H5, H3a, CH_2CH$_3$), 3.78 (dd, ^2J=9.8, ^3J=4.7 Hz, 1H; H8a), 3.65 (m, 1H; H4), 3.57 (dd, ^2J=9.8, ^3J=8.2 Hz, 1H; H8b), 3.40 (dt, ^3J=8.6, 4.7 Hz, 1H; H6), 2.40 (dd, ^3J=11.1, 8.8 Hz, 1H; H3), 1.17 (t, ^3J=7.2 Hz, 3H; CH$_2$CH_3), 0.39 (s, 3H; SiMe), 0.38 ppm (s, 3H; SiMe); ^{13}C NMR (50 MHz, $CDCl_3$, 25°C): δ=170.8 (s; C=O), 138.4–137.1 (s, 4C; C-Ar), 134.1–127.5 (d, 20C; C-Ar), 85.3 (d; C5), 83.9 (d; C4), 80.7 (d; C2), 73.4 (t; Bn), 72.7 (d; C6), 71.8 (d; C3a), 71.6, 71.1 (t, 2C; Bn), 70.8 (t; C8), 61.1 (t; CH_2CH$_3$), 36.9 (d; C3), 14.0 (q; CH$_2$CH_3), −2.7, −4.2 ppm (q, 2C; SiMe$_2$); IR ($CDCl_3$): $\tilde{\nu}$=3688, 3029, 3012, 2930, 1739, 1496, 1454, 1253 cm^{-1}; MS (70 eV): m/z (%): 560 (2), 400 (53), 296 (65), 188 (40), 181 (60), 105 (48), 91 (100); elemental analysis calcd (%) for $C_{39}H_{45}NO_6Si$ (651.3): C 71.86, H 6.96, N 2.15; found: C 71.58, H 7.13, N 2.08.

(1*R*,2*R*,3*R*,6*S*,7*S*,7a*S*)-1,2-Bis(benzyloxy)-3-[(benzyloxy)methyl-7-[dimethyl(phenyl)silyl]-6-hydroxyhexahydro-5*H*-pyrrolizin-5-one (9): A mixture of **8** (484 mg, 0.74 mmol) and Zn dust (244 mg) in CH$_3$COOH/H$_2$O 9:1 (8 mL) was heated to 60–65°C for 5 h and then filtered through cotton. The solution was cooled to 0°C and, under vigorous stirring, a saturated aqueous solution of $NaHCO_3$ (60 mL) was added until alkaline pH was reached. The aqueous phase was extracted with AcOEt (3× 60 mL) and the combined organic phases were dried over Na_2SO_4. After filtration and evaporation under reduced pressure, a viscous oil was obtained. Purification on silica gel (petroleum ether/ethyl acetate 3:2) afforded pure **9** (420 mg, 0.69 mmol, 93%) as a colorless viscous oil. R_f= 0.4 (petroleum ether/ethyl acetate 3:2). $[\alpha]_D^{22}=-47.0$ (c=1.87 in $CHCl_3$); ^{1}H NMR (400 MHz, $CDCl_3$, 25°C): δ=7.55–7.53 (m, 2H; H-Ar), 7.38–7.23 (m, 16H; H-Ar), 7.14–7.12 (m, 2H; H-Ar), 4.55 (d, ^2J=11.7 Hz, 1H; Bn), 4.46 (s, 2H; Bn), 4.38–4.34 (m, 2H; Bn, H3), 4.30 (d, ^3J=11.1 Hz, 1H; H6), 4.22 (d, ^2J=11.3 Hz, 1H; Bn), 4.12–4.09 (m, 2H; H2, Bn), 3.62 (dd, ^3J=9.8, 4.1 Hz, 1H; H7a), 3.58–3.56 (m, 1H; H1), 3.47 (dd, ^2J=9.6, ^3J=5.8 Hz, 1H; H8a), 3.43 (dd, ^2J=9.6, ^3J=8.0 Hz, 1H; H8b), 2.75 (br s, 1H; OH), 1.63 (dd, ^3J=11.1, 9.8 Hz, 1H; H7), 0.44 (s, 3H; SiMe), 0.39 ppm (s, 3H; SiMe); ^{13}C NMR (50 MHz, $CDCl_3$, 25°C): δ=176.6 (s; C5), 138.0–136.3 (s, 4C; C-Ar), 134.3–127.7 (d, 20C; C-Ar), 89.0 (d; C1), 84.4 (d; C2), 73.9 (d; C6), 73.0, 72.0, 71.5 (t, 3C; Bn), 68.5 (t; C8), 63.2 (d; C7a), 59.1 (d; C3), 38.9 (d; C7), −3.6, −4.8 ppm (q, 2C; SiMe$_2$); IR ($CDCl_3$): $\tilde{\nu}$=3400, 3000, 2850, 1700 cm^{-1}; MS (70 eV): m/z (%): 516 (4), 289 (26), 181 (13), 135 (89), 91 (100); elemental analysis calcd (%) for $C_{37}H_{41}NO_5Si$ (607.81): C 73.11, H 6.80, N 2.30; found: C 72.78, H 6.81, N 2.15.

(1*R*,2*R*,3*R*,6*S*,7*S*,7a*R*)-1,2-Bis(benzyloxy)-3-[(benzyloxy)methyl]-6,7-dihydroxyhexahydro-1*H*-pyrrolizine (10): Mercuric trifluoroacetate (64 mg, 0.15 mmol) was added to a stirred solution of **9** (47 mg, 0.079 mmol) in $CHCl_3$ (0.47 mL), acetic acid (0.12 mL) and trifluoroacetic acid (0.23 mL). The solution was stirred at RT for 1 h; then, peracetic acid (1.35 mL) was added dropwise to the mixture with ice cooling. After 1 h stirring at room temperature the solution was cooled to −10°C and a saturated aqueous solution of $Na_2S_2O_3$ (10 mL) was added dropwise. The mixture was extracted with AcOEt (3×30 mL) and the combined organic layers were washed with a saturated aqueous solution of Na_2CO_3 (30 mL), dried over anhydrous Na_2SO_4, filtered and evaporated under reduced pressure. Purification of the residue by flash column chromatography on silica gel (petroleum ether/ethyl acetate 2:3) afforded pure **10** (29 mg, 0.06 mmol, 76%) as a colorless oil. R_f=0.2 (petroleum ether/ethyl acetate 2:3). $[\alpha]_D^{20}=-41.5$ (c=0.68 in $CHCl_3$); ^{1}H NMR (400 MHz, $CDCl_3$, 25°C): δ=7.36–7.20 (m, 15H; H-Ar), 4.71 (d, ^2J=11.7 Hz, 1H; Bn), 4.56–4.42 (m, 6H; Bn, H6), 4.26 (t, ^3J=3.6 Hz, 1H; H2), 4.15–4.12 (m, 2H; H7, H3), 3.91 (t, ^3J=4.7 Hz, 1H; H1), 3.66 (t, ^3J=6.3 Hz, 1H; H7a), 3.58 (dd, ^2J=9.7, ^3J=5.8 Hz, 1H; H8a), 3.50 ppm (dd, ^2J=9.7, ^3J= 4.3 Hz, 1H; H8b); ^{13}C NMR (50 MHz, $CDCl_3$, 25°C): δ=172.6 (s; C5), 137.9–137.7 (s, 3C; C-Ar), 128.5–127.8 (d, 15 C; C-Ar), 86.9 (d; C1), 85.1 (d; C2), 80.5 (d; C7), 78.3 (d; C6), 73.3 (t; Bn), 72.1 (t, 2C; Bn), 68.3 (t; C8), 66.8 (d; C7a), 59.0 ppm (d; C3); IR ($CDCl_3$): $\tilde{\nu}$=3372, 3011, 2866, 1703, 1454, 1214, 1102 cm^{-1}; MS (70 eV): m/z (%): 428 (11), 398 (4), 368 (3) [M^+−CH$_2$OBn], 292 (20), 262 (12), 171 (90), 169 (57), 90 (100); elemental analysis calcd (%) for $C_{29}H_{31}NO_6$ (489.56): C 71.15, H 6.38, N, 2.86; found: C 70.90, H 6.31, N 2.80.

(1*R*,2*R*,3*R*,6*S*,7*S*,7a*R*)-1,2-Bis(benzyloxy)-3-[(benzyloxy)methyl]-6,7-dihydroxyhexahydro-1*H*-pyrrolizine (11): To a cooled (0°C) solution of **10** (173 mg, 0.35 mmol) in dry THF (4.2 mL) a 1 M solution of $LiAlH_4$ in THF (1.3 mL, 1.3 mmol) was added under nitrogen atmosphere. The mixture was then refluxed for 2 h. After cooling to 0°C, a saturated Na_2SO_4 solution (600 μL) was added dropwise. The suspension was then filtered through Celite and washed with AcOEt. Evaporation under reduced pressure afforded a viscous oil, that was quickly filtered over a short pad of silica gel (ethyl acetate) obtaining pure **11** as a viscous oil (130 mg, 0.27 mmol, 78%). R_f=0.6 (ethyl acetate). $[\alpha]_D^{20}=-2.9$ (c=0.53 in $CDCl_3$); ^{1}H NMR (400 MHz, $CDCl_3$, 25°C): δ=7.32–7.23 (m, 15H; H-Ar), 4.66–4.61 (m, 2H; Bn), 4.56–4.49 (m, 4H; Bn), 4.13–4.10 (m, 2H; H1, H6), 4.04 (t, ^3J=5.6 Hz, 1H; H2), 3.96 (t, ^3J=5.1 Hz, 1H; H7), 3.51 (dd, ^2J=9.6, ^3J=5.3 Hz, 1H; H8a), 3.46 (dd, ^2J=9.6, ^3J=6.3 Hz, 1H; H8b), 3.40 (dd, ^2J=11.0, ^3J=5.6 Hz, 1H; H5a), 3.36 (t, ^3J=5.3 Hz, 1H;

 © 2009 Wiley-VCH Verlag GmbH & Co. KGaA, Weinheim

H7a), 3.24 (dt, $^3J=5.6$, 5.5 Hz, 1H; H3), 2.81 ppm (dd, $^2J=11.0$, $^3J=5.3$ Hz, 1H; H5b); ^{13}C NMR (50 MHz, $CDCl_3$, 25 °C): $\delta=138.2$–137.9 (s, 3 C; C-Ar), 128.4–127.5 (d, 15 C; C-Ar), 86.8 (d; C1), 85.2 (d; C2), 81.1 (d; C7), 78.7 (d; C6), 73.6 (d; C7a), 73.3 (t; Bn), 72.5 (t; Bn), 72.0 (t; Bn), 71. 6 (t; C8), 69.8 (d; C3), 59.9 ppm (t; C5); IR ($CDCl_3$): $\tilde{\nu}=3393$, 2870, 2246, 1711, 1596, 1495, 1453, 1362, 1101; MS (70 eV): *m/z* (%): 354 (38) [M^+-CH_2OBn], 234 (3), 172 (18), 160 (12), 91 (100); elemental analysis calcd (%) for $C_{29}H_{33}NO_5$ (475.58): C 73.24, H 6.99, N 2.95; found: C 72.98, H 7.23, N 2.83.

(1*R*,2*R*,3*R*,6*S*,7*S*,7a*R*)-3-(Hydroxymethyl)hexahydro-1*H*-pyrrolizine-1,2,6,7-tetrol (casuarine, 1): To a stirred solution of **11** (89 mg, 0.19 mmol) in MeOH (12.5 mL), 4–5 drops of conc. HCl and 100 mg of Pd (10% on C) were added. The suspension was stirred under hydrogen atmosphere for 4 d, then filtered through Celite and washed with MeOH. Evaporation under reduced pressure afforded a vitreous solid that was transferred to a column of DOWEX 50WX8 and then washed with MeOH (15 mL), H_2O (10 mL) to remove non amine containing products and then with 7% NH_4OH (25 mL) to elute casuarine (**1**). Evaporation of the solvent afforded casuarine as a white solid (39 mg, 0.19 mmol, 100%). M.p. 180–182 °C; $[\alpha]_D^{20}=+14.4$ ($c=0.52$ in H_2O); ^{1}H NMR (400 MHz, D_2O, 25 °C): $\delta=4.19$–4.13 (m, 2H; H6, H7), 4.15 (t, $^3J=8.2$ Hz, 1H; H1), 3.80–3–75 (m, 2H; H2, H8a), 3.60 (dd, $^2J=11.7$, $^3J=6.6$ Hz, 1H; H8b), 3.27 (dd, $^2J=11.8$, $^3J=3.7$ Hz, 1H; H5a), 3.10 (dd, $^3J=8.5$, 2.5 Hz, 1H; H7a), 3.07–3.04 (m, 1H; H3), 2.94 ppm (dd, $^2J=11.8$, $^3J=3.0$ Hz, 1H; H5b); ^{13}C NMR (50 MHz, D_2O, 25 °C): $\delta=78.9$ (d; C7), 77.8 (d; C1), 77.6 (d; C6), 76.6 (d; C2), 72.7 (d; C7a), 70.3 (d; C3), 62.1 (t; C8), 58.3 ppm (t; C5); IR (KBr): $\tilde{\nu}=3329$, 2917, 1650, 1416; MS (70 eV): *m/z* (%): 205 (0.9) [M^+], 188 (0.2) [M^+-H_2O], 174 (100) [M^+-CH_2OH], 128 (15), 102 (17), 70 (40); elemental analysis calcd (%) for $C_8H_{15}NO_5$ (205.21): C 46.82, H 7.37, N 6.83; found: C 46.51, H 7.54, N 6.73.

(2,3,4,6-Tetra-*O*-benzyl-α-D-glucopyranosyl)-(1→6)-*O*-tetra(benzyloxy)-5-oxo-casuarine (15): A solution of glucopyranosyl tricholoroacetimidate (**14**, 230 mg, 0.33 mmol) and pyrrolizidine **13** (115 mg, 0.20 mmol) in dry diethyl ether (4 mL) was stirred for 10 min at room temperature under nitrogen atmosphere in the presence of 3 Å molecular sieves (150 mg). After cooling to −20 °C and addition of trimethylsilyl trifluoromethanesulfonate (18 μL, 0.10 mmol), stirring was continued for 40 min; during this period the temperature was raised to RT. The mixture was washed with a sat. Na_2CO_3 solution (2 mL), dried over Na_2SO_4, filtered and concentrated to dryness. The residue was purified by flash column chromatography on silica gel (petroleum ether/ethyl acetate 5:1) to afford pure **15** (159 mg, 0.144 mmol, 72%) as a colorless oil. $R_f=0.32$ (petroleum ether/ethyl acetate 5:1). $[\alpha]_D^{24}=+51.5$ ($c=0.87$ in $CHCl_3$); ^{1}H NMR (400 MHz, $CDCl_3$, 25 °C): $\delta=7.47$–7.12 (m, 40H; H-Ar), 5.69 (d, $^3J=3.5$ Hz, 1H; H1), 5.01 (d, $^2J=10.8$ Hz, 1H; Bn), 5.00 (d, $^2J=11.9$ Hz, 1H; Bn), 4.84 (d, $^2J=10.9$ Hz, 1H; Bn), 4.77 (d, $^2J=10.8$ Hz, 1H; Bn), 4.75 (d, $^2J=10.5$ Hz, 1H; Bn), 4.73 (d, $^3J=8.2$ Hz, 1H; H6′), 4.64–4.32 (m, 11H; Bn), 4.31 (dd, $^3J=4.1$, 3.7 Hz, 1H; H2′), 4.21–4.17 (m, 2H; H3′, H7′), 3.99 (dd, $^3J=9.4$, 9.2 Hz, 1H; H4), 3.99–3.94 (m, 2H; H5, H1′), 3.74 (dd, $^3J=6.6$, 6.4 Hz, 1H; H7a′), 3.68 (dd, $^3J=9.6$, 9.2 Hz, 1H; H3), 3.64 (dd, $^3J=9.6$, 3.5 Hz, 1H; H2), 3.61–3.53 (m, 3H; H6a, H8′a, H8′b), 3.45 ppm (dd, $^2J=10.7$, $^3J=1.7$ Hz, 1H; H6b); ^{13}C NMR (50 MHz, $CDCl_3$, 25 °C): $\delta=169.4$ (s; C5′), 138.9–137.2 (s, 8 C; C-Ar), 128.5–127.5 (d, 40 C; C-Ar), 95.2 (d; C1), 87.2 (d; C1′), 86.1 (d; C2′), 84.4 (d; C7′), 81.6 (d; C4), 78.6 (d; C2), 77.9 (d; C6′), 77.3 (d; C3), 75.7, 74.9 (t, 2 C; Bn), 73.3 (t, 2C; Bn), 72.3 (t; Bn), 72.0 (t, 2 C; Bn), 71.7 (t; Bn), 70.4 (d; C5), 69.2 (t; C8′), 68.1 (t; C6), 65.8 (d; C7a′), 58.9 ppm (d; C3′); IR ($CHCl_3$): $\tilde{\nu}=3066$, 3032, 3010, 2867, 1711, 1454, 1098 cm^{-1}; HRMS (ESI): *m/z*: calcd for $C_{70}H_{71}NO_{11}Na$ [M+Na]$^+$: 1124.4919; found: 1124.4918; elemental analysis calcd (%) for $C_{70}H_{71}NO_{11}$ (1102.31): C 76.27, H 6.49, N 1.27; found: C 76.53, H 6.76, N 1.38.

(2,3,4,6-Tetra-*O*-benzyl-α-D-glucopyranosyl)-(1→6)-*O*-tetra(benzyloxy)-casuarine (16): To a solution of **15** (300 mg, 0.27 mmol) in dry THF (8.0 mL) a 2 M solution of $LiBH_4$ in THF (2.01 mL, 4.05 mmol) and 1 M BH_3 in THF (4.05 mL, 4.05 mmol) were added dropwise at 0 °C. The reaction mixture was stirred at 23 °C for 3 d, then, after cooling to −15 °C, H_2O (3 mL) was added dropwise. The THF was then evaporated and the mixture was filtered and extracted with Et_2O. The organic layer was dried over Na_2SO_4, filtered and concentrated to dryness. The residue was purified by flash column chromatography on silica gel (petroleum ether/ethyl acetate 4:1) to afford pure **16** (199 mg, 0.18 mmol, 68%) as a colorless oil. $R_f=0.38$ (petroleum ether/ethyl acetate 4:1); $[\alpha]_D^{24}=+20.3$ ($c=0.60$ in $CDCl_3$); ^{1}H NMR (400 MHz, $CDCl_3$, 25 °C): $\delta=7.29$–7.14 (m, 40H; H-Ar), 4.84–4.78 (m, 3H; H1 + 2 Bn), 4.71 (d, $^2J=11.7$ Hz, 1H; Bn), 4.68–4.64 (m, 2H; Bn), 4.55–4.34 (m, 12H; 11 Bn + 1H), 4.22 (d, $J=11.3$ Hz, 1H), 4.16–4.09 (m, 3H; H2′ + 2H), 3.98–3.84 (m, 3H; H1′, H5′a + 1H), 3.76 (t, $J=9.3$ Hz; 1H), 3.64–3.41 ppm (m, 7H; H5′b + 6H); ^{13}C NMR (50 MHz, $CDCl_3$, 25 °C): $\delta=138.2$–137.0 (s, 8 C; C-Ar), 128.6–127.2 (d, 40 C; C-Ar), 95.1 (d; C1), 85.7 (d, C1′), 83.6 (d; C2′), 81.4 (d; 3C), 80.3, 78.9, 77.2 (d; 3C), 75.3, 74.9, 73.4, 73.0, 72.7, 72.4, 71.8, 70.9 (t, 8C; Bn), 71.4, 69.3 (d; 2C), 68.3, 67.5 (t, 2C; C6, C8′), 65.3 ppm (t; C5′); IR ($CHCl_3$): $\tilde{\nu}=3676$, 3513, 3010, 2921, 2869, 2388, 1951, 1876, 1811, 1603, 1497, 1454, 1364, 1215, 1086, 1072 cm^{-1}; HRMS (ESI): *m/z*: calcd for $C_{70}H_{74}NO_{10}$ [M+H]$^+$: 1188.5307; found: 1188.5296; elemental analysis calcd (%) for $C_{70}H_{73}NO_{10}$ (1088.33): C 77.25, H 6.76, N 1.29; found: C 76.72, H 6.91, N 1.15.

6-α-D-Glucopyranosyl-*O*-casuarine (2): A solution of **16** (196 mg, 0.18 mmol) in MeOH (25 mL) was stirred at room temperature under H_2 atmosphere for 24 h in the presence of 10% Pd/C (350 mg) and 4–5 drops of conc. HCl. Filtration through Celite afforded a waxy solid that was transferred to a column of DOWEX 50WX8 and then washed with MeOH (15 mL), H_2O (10 mL) to remove non amine containing products and then with 7% NH_4OH (25 mL) to elute pure **2** (50 mg, 0.14 mmol, 77%) as a white foam. An analytically pure sample was obtained by filtration through DOWEX 50WX8–200. $[\alpha]_D^{23}=+91.9$ ($c=0.35$ in H_2O); ^{1}H NMR (400 MHz, D_2O, 25 °C): $\delta=4.89$ (d, $^3J=3.7$ Hz, 1H; H1), 4.24 (t, $^3J=3.0$ Hz, 1H; H7′), 4.09 (dt, $^3J=4.3$, 3.0 Hz, 1H; H6′), 4.00 (t, $^3J=8.2$ Hz, 1H; H1′), 3.79–3.75 (m, 1H; H6a), 3.68–3.56 (m, 5H; H3, H5, H6b, H2′, H8′a), 3.49 (dd, $^2J=11.8$, $^3J=6.3$ Hz, 1H; H8′b), 3.47 (dd, $^3J=10.0$, 3.7 Hz, 1H; H2), 3.31 (t, $^3J=9.4$ Hz, 1H, H4), 3.13 (dd, $^2J=12.9$, $^3J=4.3$ Hz, 1H; H5′a), 3.01–2.96 ppm (m, 3H; H3′, H5′b, H7a′); ^{13}C NMR (50 MHz, D_2O, 25 °C): $\delta=96.7$ (d; C1), 83.0 (d; C6′), 77.4 (d; C7′), 76.9 (d; C1′), 76.1 (d; C2′), 72.1 (d; C7a′), 71.9 (d; C3), 71.5 (d; C5), 70.3 (d; C2), 68.9 (d; C4), 68.6 (d; C3′), 62.0 (t; C8′), 59.8 (t; C6), 55.1 ppm (t; C5′); HRMS (ESI): *m/z*: calcd for $C_{14}H_{26}NO_{10}$ [M+H]$^+$: 368.1551; found: 368.1544; elemental analysis calcd (%) for $C_{14}H_{25}NO_{10}$ (367.35): C 45.77, H 6.86, N 3.81; found: C 45.39, H 6.57, N 3.46.

Kinetic methods: Inhibition assays of NtMGAM were carried out in 96-well microtitre plates containing 100 mM MES buffer, pH 6.5, inhibitor and *p*-nitrophenol D-glucopyranoside (*p*NP-glucose, Sigma) as substrate (2.5–30 mM). The reaction was allowed to proceed for 50 minutes at 37 °C before quenching with 0.5 M sodium carbonate and measuring the release of the *p*-nitrophenolate ion at 405 nm.

Inhibition of Tre37A was determined using a stopped assay, where glucose was detected using glucose oxidase/peroxidase linking enzymes (Megazyme, Bray, Eire) in the same way as described previously.[11] Measurements were made at trehalose concentrations between 0.05 and 6 mM and Tre37A was present at a final concentration of 0.7 nM.

The K_i values of **1** and **2** against NtMGAM and Tre37A were calculated by determining the reaction rates of the enzymes in the absence and presence of inhibitor. Concentrations of 0.2–0.6 μM **1** or 0.4–1.2 mM **2** were used to inhibit NtMGAM and concentrations of 10–40 μM **1** or 10–20 nM **2** were used to inhibit Tre37A. Rates were determined and the data fitted to the Michaelis–Menten equation in GRAFIT (Erithacus Software Ltd., Horley, UK) to obtain a K_M (in absence of inhibitor) or apparent K_M (K_M^{app}) (in presence of inhibitor). K_i values were determined using the equation $K_M^{app}=K_M(1+[I]/K_i)$.

Structural methods: The crystallization of NtMGAM was previously reported by Sim et al.[9] The complex of NtMGAM with **1** was obtained by soaking NtMGAM crystals for ≈12 h in mother liquor supplemented with 200 μM **1**. X-ray diffraction data were collected on an ADSC Quantum-4 CCD detector at beamline F1 at the Cornell High Energy Synchrotron Source (CHESS) and were processed with HKL2000.[28] Since the crystal of NtMGAM in complex with **1** was isomorphous to the crystal of NtMGAM in complex with acarbose,[9] this structure was used as

 © 2009 Wiley-VCH Verlag GmbH & Co. KGaA, Weinheim

an initial model to calculate F_o-F_c maps. These difference maps clearly revealed the position of casuarine in the NtMGAM active site. Inhibitor topologies and restraints were generated using the PRODRG server (http://davapc1.bioch.dundee.ac.uk/programs/prodrg/) and the model was subsequently modified and refined using COOT[29] and REFMAC.[30] Data processing and refinement statistics are shown in Table 2.

Table 2. Data collection and refinement statistics.

Crystal	NtMGAM in complex with **1**	Tre37A in complex with **2**
space group	$P2_12_12_1$	$P2_12_12_1$
unit cell dimensions		
a [Å]	86.7	92.5
b [Å]	109.1	117.9
c [Å]	109.4	203.5
data collection[a]		
beamline	CHESS F1	ESRF ID29
λ [Å]	0.9175	0.9700
resolution range [Å]	16–2.1	20–1.9
unique reflections	57768	174266
redundancy	6.3 (5.5)	7.1 (5.9)
$I/\sigma I$	11.9 (5.0)	18.9 (2.8)
completeness [%]	95.6 (97.4)	99.6 (96.2)
R_{sym}	0.118 (0.432)	0.098 (0.524)
refinement statistics		
R_{cryst} [%]	22.5	17.7
R_{free} [%]	27.8	22.4
R.M.S.D. bonds [Å]	0.014	0.012
R.M.S.D. angles [°]	1.53	1.38
PDB code	3CTT	2JJB

[a] Values in parentheses refer to the highest-resolution shell; R.M.S.D., root mean square deviation.

Gene expression and purification of Tre37A was carried out as described previously.[11] Protein, at a concentration of 10–12 mg/mL, was co-crystallized with 5 mM **2** from 1.7 M ammonium sulfate and 0.1 M citric acid buffer, pH 3.5. Crystals were cryoprotected in the mother liquor supplemented with 25% ethylene glycol and flash frozen. Data were collected on beamline ID29 at the European Synchrotron Radiation Facility (ESRF), and were processed with the HKL2000 suite.[28] As the cell dimensions differed from previous complexes of Tre37A, structure solution required molecular replacement in PHASER[31] using a monomer of 2JF4 as the search model. The model was refined with manual building in COOT[29] interspersed with refinement of geometric restraints in REFMAC.[30] Data processing and refinement statistics are shown in Table 2.

Computational methods: All calculations were performed on 2×AMD Opteron285 Dual Core processors running Linux RedHat OS. The structures of the complexes between NtMGAM and casuarine (**1**) and Tre37A and casuarine 6-*O*-α-glucoside (**2**) were superimposed by the pyrrolizidine nuclei. After the removal of all non-protein molecules, the crystallographic structures were prepared according to the Glide protein preparation procedure[26] used to assign missing hydrogens and to reduce structural problems. Docking calculations were performed with the Glide program using default input parameters (no scaling factor for the vdW radii of non polar protein atoms, 0.8 scaling factor for non polar ligand atoms) and the SP scoring function was used to evaluate the resulting poses. The best docked conformations were chosen using the GlideScore, a modified and extended version of the empirically based ChemScore function.[32]

Acknowledgements

We thank MiUR and Ente Cassa di Risparmio di Firenze, Italy, for financial support. Ente CRF is also acknowledged for granting a 400 MHz NMR spectrometer. Brunella Innocenti and Maurizio Passaponti (Dipartimento di Chimica Organica "U. Schiff") are acknowledged for technical assistance. CINMPIS is gratefully acknowledged for a grant to C.P. L.S. holds a scholarship from NSERC Canada and D.R.R. grants from CIHR (MOP79400) and Heart and Stroke Canada (NA-6305). The York laboratory would like to thank the BBSRC for funding. G.J.D. is a recipient of a Royal Society/Wolfson Research Merit award. T.M.G. is a Sir Henry Wellcome postdoctoral fellow. The Cornell High Energy Synchrotron Source (CHESS), is supported by the National Science Foundation under award DMR-0225180, and the Macromolecular Diffraction at CHESS (MacCHESS) facility, by award RR-01646 from the National Institutes of Health, through its National Center for Research Resources.

[1] a) R. J. Nash, P. I. Thomas, R. D. Waigh, G. W. J. Fleet, M. R. Wormald, P. M. De Q. Lilley, D. J. Watkin, *Tetrahedron Lett.* **1994**, *35*, 7849–7852; b) M. R. Wormald, R. J. Nash, A. A. Watson, B. K. Bhadoria, R. Langford, A. Sims, G. W. J. Fleet, *Carbohydr. Lett.* **1996**, *2*, 169–174.

[2] a) R. N. Chopra, S. L. Nayar, I. C. Chopra, *Glossary of Indian Medicinal Plants*, Council of Scientific and Industrial Research (India), New Dehli, **1956**, p. 55; b) R. B. Nair, G. Santhakumari, *Ancient Science of Life: Journal of International Institute of Ayurveda* **1986**, *6*, 80–84.

[3] a) J. K. Grover, S. Yadav, V. Vats, *J. Ethnopharmacol.* **2002**, *81*, 81–100; b) S. R. Mentreddy, *J. Sci. Food Agric.* **2007**, *87*, 743–750.

[4] A. Kato, E. Kano, I. Adachi, R. J. Molyneux, A. A. Watson, R. J. Nash, G. W. J. Fleet, M. R. Wormald, H. Kizu, K. Ikeda, N. Asano, *Tetrahedron: Asymmetry* **2003**, *14*, 325–331.

[5] P. M. Coutinho, B. Henrissat in *Recent Advances in Carbohydrate Bioengineering* (Eds.: H. J. Gilbert, G. J. Davies, B. Henrissat, B. Svensson), Royal Society of Chemistry, Cambridge, **1999**, pp. 3–12.

[6] a) B. L. Nichols, J. Eldering, S. Avery, D. Hahn, A. Quaroni, E. E. Sterchi, *J. Biol. Chem.* **1998**, *273*, 3076–3081; b) B. L. Nichols, S. Avery, P. Sen, D. M. Swallow, D. Hahn, E. E. Sterchi, *Proc. Natl. Acad. Sci. USA* **2003**, *100*, 1432–1437.

[7] N. Asano, *Glycobiology* **2003**, *13*, 93R–104R.

[8] For reviews on glycosidase mechanisms, see: a) T. D. Heightman, A. T. Vasella, *Angew. Chem.* **1999**, *111*, 794–815; *Angew. Chem. Int. Ed.* **1999**, *38*, 750–770; b) D. L. Zechel, S. G. Withers, *Acc. Chem. Res.* **2000**, *33*, 11–18; c) C. S. Rye, S. G. Withers, *Curr. Opin. Chem. Biol.* **2000**, *4*, 573–580.

[9] L. Sim, R. Quezada-Calvillo, E. E. Sterchi, B. L. Nichols, D. R. Rose, *J. Mol. Biol.* **2008**, *375*, 782–792.

[10] J. Defaye, H. Driguez, B. Henrissat, *Carbohydr. Res.* **1983**, *124*, 265–273.

[11] R. P. Gibson, T. M. Gloster, S. Roberts, R. A. J. Warren, I. S. de Gracia, A. García, J. L. Chiara, G. J. Davies, *Angew. Chem.* **2007**, *119*, 4193–4197; *Angew. Chem. Int. Ed.* **2007**, *46*, 4115–4119.

[12] a) S. E. Denmark, A. R. Hurd, *Org. Lett.* **1999**, *1*, 1311–1314; b) S. Denmark, A. R. Hurd, *J. Org. Chem.* **2000**, *65*, 2875–2886; c) I. Izquierdo, M. T. Plaza, J. A. Tamayo, *Tetrahedron* **2005**, *61*, 6527–6533; d) R. J. Nash, G. W. J. Fleet, J. Van Ameijde, G. Horne, *PCT Int. Appl.*, WO2006008493, **2006**.

[13] Casuarine has also been obtained as a side-product during the synthesis of targeted 3-*epi*-casuarine: a) J. Van Ameijde, G. Horne, M. R. Wormald, R. A. Dwek, R. J. Nash, P. W. Jones, E. L. Evinson, G. W. J. Fleet, *Tetrahedron: Asymmetry* **2006**, *17*, 2702–2712. For related syntheses of casuarine diastereoisomers, see also: b) ref. [12d]; c) I. Izquierdo, M. T. Plaza, J. A. Tamayo, *J. Carbohydr. Chem.* **2006**, *25*, 281–295; d) T. Ritthiwigrom, S. G. Pyne, *Org. Lett.* **2008**, *10*, 2769–2771.

[14] N. Asano, T. Yamauchi, K. Kagamifuchi, N. Shimizu, A. Takahashi, H. Takatsuka, K. Ikeda, H. Kizu, W. Chuakul, A. Kettawan, T. Okamoto, *J. Nat. Prod.* **2005**, *68*, 1238–1242.

[15] Chemical syntheses of glycosyl iminosugars: a) P. B. Anzeveno, L. J. Creemer, J. K. Daniel, C.-H. R. King, P. S. Liu, *J. Org. Chem.* **1989**, *54*, 2539–2542; b) P. S. Liu, J. K. Daniel, B. L. Rhinehart, *Eur. Pat. Appl.* EP297534, **1989** [*Chem. Abstr.* **1989**, *111*, 7659r]; c) H.

 © 2009 Wiley-VCH Verlag GmbH & Co. KGaA, Weinheim

Ardron, T. D. Butters, F. M. Platt, M. R. Wormald, R. A. Dwek, G. W. J. Fleet, G. S. Jacob, *Tetrahedron: Asymmetry* **1993**, *4*, 2011–2024; d) F.-X. Felpin, K. Boubekeur, J. Lebreton, *J. Org. Chem.* **2004**, *69*, 1497–1503.

[16] Enzymatic syntheses of glycosyl iminosugars: a) N. Asano, K. Oseki, E. Kaneko, K. Matsui, *Carbohydr. Res.* **1994**, *258*, 255–266; b) N. Asano, A. Kato, H. Kizu, K. Matsui, R. C. Griffiths, M. G. Jones, A. A. Watson, R. J. Nash, *Carbohydr. Res.* **1997**, *304*, 173–178.

[17] F. Cardona, E. Faggi, F. Liguori, M. Cacciarini, A. Goti, *Tetrahedron Lett.* **2003**, *44*, 2315–2318.

[18] P. DeShong, J. M. Leginus, S. W. Lander Jr, *J. Org. Chem.* **1986**, *51*, 574–576.

[19] J. Revuelta, S. Cicchi, A. Goti, A. Brandi, *Synthesis* **2007**, *4*, 485–504.

[20] A. Goti, S. Cicchi, M. Cacciarini, F. Cardona, V. Fedi, A. Brandi, *Eur. J. Org. Chem.* **2000**, 3633–3645.

[21] For our related work on the synthesis of necine bases, see: a) A. Goti, V. Fedi, L. Nannelli, F. De Sarlo, A. Brandi, *Synlett* **1997**, 577–579; b) A. Goti, M. Cacciarini, F. Cardona, F. M. Cordero, A. Brandi, *Org. Lett.* **2001**, *3*, 1367–1369.

[22] a) K. Tamao, N. Ishida, T. Tanaka, M. Kumada, *Organometallics* **1983**, *2*, 1694–1696; b) K. Tamao, N. Ishida, *J. Organomet. Chem.* **1984**, *269*, C37-C39; c) I. Fleming, R. Henning, H. E. Plaut, *J. Chem. Soc. Chem. Commun.* **1984**, 29–31; d) I. Fleming, R. Henning, D. C. Parker, H. E. Plaut, P. E. J. Sanderson, *J. Chem. Soc. Perkin Trans. 1* **1995**, 317–337.

[23] S. Nukui, M. Sodeoka, H. Sasai, M. Shibasaki, *J. Org. Chem.* **1995**, *60*, 398–404.

[24] R. Quezada-Calvillo, L. Sim, Z. Ao, B. R. Hamaker, A. Quadroni, G. D. Brayer, E. E. Sterchi, C. C. Robayo-Torres, D. R. Rose, B. L. Nichols, *J. Nutr.* **2008**, *138*, 685–692.

[25] R. M. Esnouf, *J. Mol. Graph. Model* **1997**, *15*, 132–134.

[26] a) R. A Friesner, J. L. Banks, R. B. Murphy, T. A. Halgren, J. Klicic, D. T. Mainz, M. P. Repasky, E. H. Knoll, M. Shelley, J. K. Perry, D. Shaw, P. Francis, P. S. Shenkin, *J. Med. Chem.* **2004**, *47*, 1739–1749; b) Schrödinger, LLC, New York (http://www.schrodinger.com).

[27] A. C. Wallace, R. A. Laskowski, J. M. Thornton, *Prot. Eng.*, **1995**, *8*, 127–134.

[28] Z. Otwinowski, W. Minor, *Methods Enzymol.* **1997**, *276*, 307–326.

[29] P. Emsley, K. Cowtan, *Acta Crystallogr. Sect. A* **2004**, *60*, 2126–2132.

[30] G. N. Murshudov, A. A. Vagin, E. J. Dodson, *Acta Crystallogr. Sect. A* **1997**, *53*, 240–255.

[31] A. J. McCoy, R. W. Grosse-Kunstleve, P. D. Adams, M. D. Winn, L. C. Storoni, R. J. Read, *J. Appl. Crystallogr.* **2007**, *40*, 658–674.

[32] M. D. Eldridge, C. W. Murray, T. R. Auton, G. V. Paolini, R. P. Mee, *J. Comput. Aided Mol. Des.* **1997**, *11*, 425–445.

Received: August 1, 2008
Published online: January 2, 2009

 © 2009 Wiley-VCH Verlag GmbH & Co. KGaA, Weinheim